Preprint Title	A multicomponent reaction-initiated synthesis of imidazopyridine-fused isoquinolinones
Authors	Ashutosh Nath, John M. Awad and Wei Zhang
Publication Date	20 März 2025
Article Type	Full Research Paper
Supporting Information File 1	25-3-19 SupInf.pdf; 2.9 MB
ORCID® iDs	Wei Zhang - https://orcid.org/0000-0002-6097-2763

BEILSTEIN JOURNAL OF ORGANIC CHEMISTRY

A multicomponent reaction-initiated synthesis of imidazopyridine-fused isoquinolinones

Ashutosh Nath, John Mark Awad, Wei Zhang*

Address: Department of Chemistry, University of Massachusetts Boston, MA 02125, USA

Email: Wei Zhang* - wei2.zhang@umb.edu

Keywords: Groebke-Blackburn-Bienaymé (GBB), Intramolecular Diles-Alder (IMDA), Multicomponent reaction (MCR), Re-aromatization, Imidazopyridine, Isoquinolinone

Abstract

A new synthetic route initiated with Groebke-Blackburn-Bienaymé (GBB) followed by *N*-acylation, intramolecular Diels-Alder (IMDA), and dehydrative re-aromatization reactions for the synthesis of imidazopyridine-fused isoquinolinones is developed. Gaussian computation analysis on the effect of the sunstitution groups for the IMDA reaction is analyzed to understand the reaction mechanism.

Introduction

Multicomponent reactions (MCRs) have intrinsic green chemistry advantages of synthetic efficiency and operational simplicity. Performing post-condensational modifications of MCR could generate novel and complex molecular scaffolds [1–8]. Some MCR adducts generated from the Ugi, Passerini, Gewald, and Biginelli, Groebke-Blackburn-Bienaymé (GBB) reactions have been modified to form chemically diverse heterocyclic scaffolds with potential biological activities [9].

Imidazo[1,2-*a*]pyridine and isoquinolinone-kind scaffold are privileged rings which can be found in drug molecules such as zolimidine [10], zolpidem [11], and alpidem antiemetic drug 5-HT3A antagonist palonosetron [12] (Figure 1). Imidazopyridine-fused isoquinolinones have been developed as HIV inhibitors [13]. The imidazo[1,2-*a*]pyridine ring can be readily synthesized by the GBB reaction [14], while the isoquinolinone ring is commonly generated by cyclative lactamization process. Performing GBB reaction followed by intramolecular amidation is a good approach for making imidazopyridine-fused isoquinolinones.

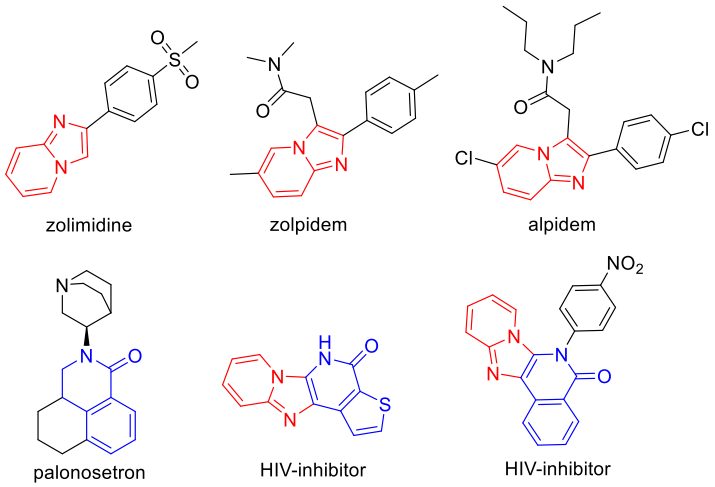

Figure 1. Bioactive compounds bearing imidazopyridine (red) and isoquinolinone-kind (blue) ring

The Veljkovic group employed methyl 2-formylbenzoate for the GBB reaction to form adducts **I** which undergoes intramolecular amidation to afford product **A** (Scheme 1, A) [15]. In a patent filed by Tibotec Pharmaceuticals, substituted alkyl isonitriles were used for the GBB reaction followed by the cleavage of the alkyl group to give intermediate **II** as a free amine. Annulation of **II** with CDI gave product **B** which is an HIV reverse transcriptase inhibitor (Scheme 1, B) [16]. We have reported a three-component [3+2] cycloaddition followed by IMDA for making heterocyclic compounds [17]. Presented in this paper is a new synthetic route involving GBB, *N*-acylation and IMDA reactions for making intermediate **III** followed by dehydrative re-aromatization to give imidazopyridine-fused isoquinolinones **C** (Scheme 1, C)**.**

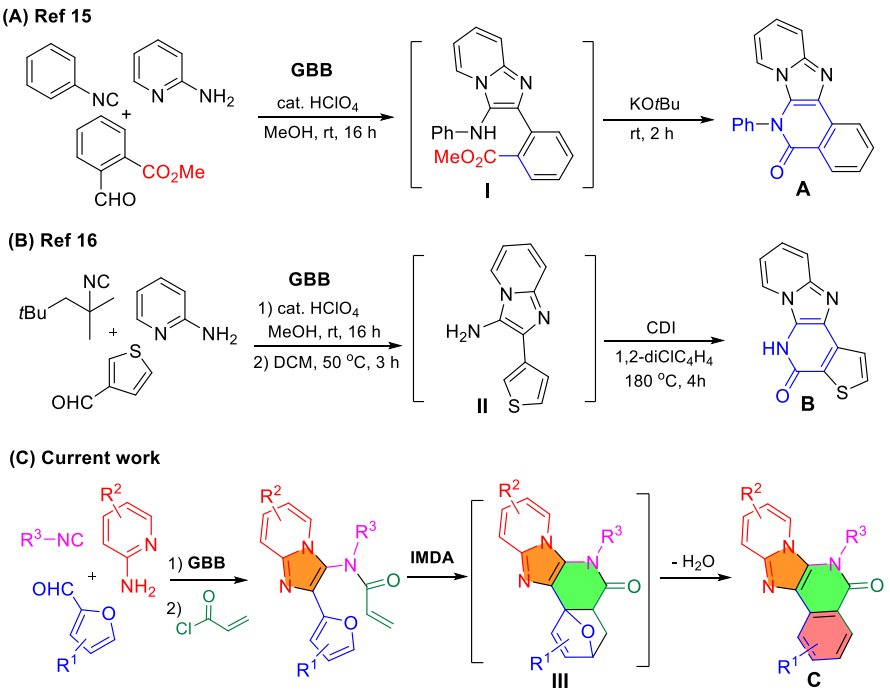

Scheme 1. GBB-initiated synthesis of imidazopyridine-fused isoquinolinones

Results and Discussion

Following the reported procedures [14], the initial GBB reaction of aminopyridines **1** (0.5 mmol), isocyanides **3** (1.2 equiv.), and furfuraldehyde **2** (1.2 equiv.) was conducted in 3:1 CH_2Cl_2:MeOH (4 mL) using $Yb(OTf)_3$ (0.08 equiv.) as a Lewis acid catalyst under microwave irradiation at 100 °C for 1 h (Scheme 2). Nineteen distinct adducts **4** were obtained in 89–98% yields. Reactions of **4** with acryloyl chloride **5** (1.5 equiv.) in the presence of Et_3N (2 equiv.) at room temperature in anhydrous CH_2Cl_2 for 6 h afforded 19 *N*-acylated compounds **6** in 80–90% yields [18].

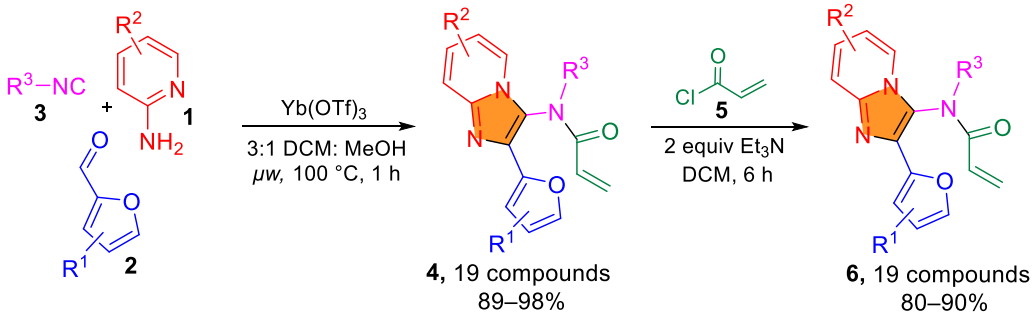

Scheme 2. The GBB reaction and *N*-acylation for making imidazo[1,2-*a*]pyridines **6**

With *N*-acylated GBB adducts **6** in hand, the synthesis of imidazopyridine-fused isoquinolinones **8** was explored by conducting IMDA and spontaneous dehydrative re-aromatization reactions. The IMDA reaction using **6a** as a model compound was systematically evaluated by varying catalysts, solvents, reaction temperatures and times (Table 1). The best conditions were found to use $AlCl_3$ as a catalyst in 1,2-dichlorobenzene at 180 °C for 4 h, which gave **8a** in 85% conversion and 82% isolated yield (entry 3). Other solvents like toluene and xylene gave minimal or no product. Different combinations of temperature and reaction time couldn't improve the yield. Among the various Lewis acids tested, $AlCl_3$ gave the best result, while CuCl, $ZnCl_2$, $PdCl_2$ and $Sc(OTf)_3$ showed moderate conversions (30–55%), and $NiCl_2$ had the lowest efficiency. During the reaction, IMDA adduct **7c** was detected by LC-MS (Figure S1), but it was not stable enough for isolation. The structure of **8a** was confirmed by single crystal X-ray diffraction analysis.

The optimized reaction condition was used to evaluate the substrate scope in the synthesis of imidazopyridine-fused isoquinolinones **8** (Table 2). The R^1 on the furan ring was found to have the most significant impact on the IMDA reaction. Br at 3- or 4-position resulted **8a** to **8i** in 66–86% yields, while Br or Me at 5-positione inhibited the IMDA reaction in making **8j** and **8k**. To understand the alignment and distance for establishing the transition state in the IMDA reaction, a comprehensive

Table 1. Optimization of IMDA and re-aromatization reactions for making **8a**

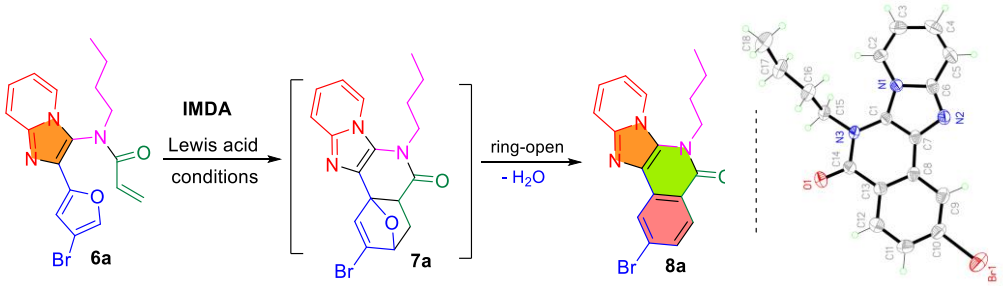

X-ray of **8a**

entry	catalyst (10 mol %)	solvent	temp (° c)	time	conversion (%)
1	$AlCl_3$	toluene	120	12 h	0
2	$FeCl_3$	1,2-dichlorobenzene	120 (μw)	1 h	0
3	**$AlCl_3$**	**1,2-dichlorobenzene**	**180**	**4 h**	**85**
4	$AlCl_3$	1,2-dichlorobenzene	180 (μw)	1 h	5
5	$AlCl_3$	1,2-dichlorobenzene	120 (μw)	2 h	15
6	$AlCl_3$	xylene	140	4 h	0
7	$ZnCl_2$	1,2-dichlorobenzene	140	4 h	50
8	CuCl	1,2-dichlorobenzene	180	4 h	55
9	$PdCl_2$	1,2-dichlorobenzene	180	4 h	40
10	CsF	1,2-dichlorobenzene	180	4 h	30
11	$Sc(OTf)_3$	1,2-dichlorobenzene	180	4 h	35
12	$CsCO_3$	1,2-dichlorobenzene	180	4 h	30
13	$InCl_3$	1,2-dichlorobenzene	180	4 h	20
14	$Yb(OTf)_3$	1,2-dichlorobenzene	180	4 h	60
15	$NiCl_2$	1,2-dichlorobenzene	180	4 h	47

DFT investigation of reactant **6** was carried out to analyze the transition state of the IMDA reaction for a Br-substituted diene and its charge distribution (Figure 2). The diene has a notable positive charge (+0.318, +0.098, **6a**), (+0.334, +0.082, **6h**) and (+0.316, +0.074, **6r**) whereas the dienophile presents a negative charge (-0.280 to -0.325, **6a**), (-0.280 to -0.327, **6h**) and (-0.280 to -0.327, **6r**), respectively. This structure induces electrostatic repulsion instead of the requisite attraction for a successful interaction between the electron-rich diene and the electron-deficient dienophile, characteristic of Diels-Alder processes. The incorporation of a bromine atom at the 5-position of the diene (+0.306, -0.041, **6j**) complicates the situation. As an electronegative element, Br exerts an inductive electron-withdrawing influence to enhance the electron shortage of the diene. This electronic imbalance reduces the diene's nucleophilicity, rendering it less reactive to the dienophile. The unfeasibility of the IMDA reaction in this system arises from inadequate interatomic distances, electrostatic repulsion from incompatible associated dienophile was conducted [18,19]. Firstly, the charge and the electronic consequences of the 5-Br substitution were considered, which were found to inhibit the system from attaining the requisite conditions for successful cycloaddition. Secondly, the interatomic distances

between the reactive centers of the diene and dienophile are almost similar for all substitutes of **6a**, **6h**, **6r** and **6j**, which, are not ideal effective for IMDA cycloaddition compare the others substitute cycloaddition.

Table 2. Substrate scope for IMDA and dehydrative aromatization in making **8**[a]

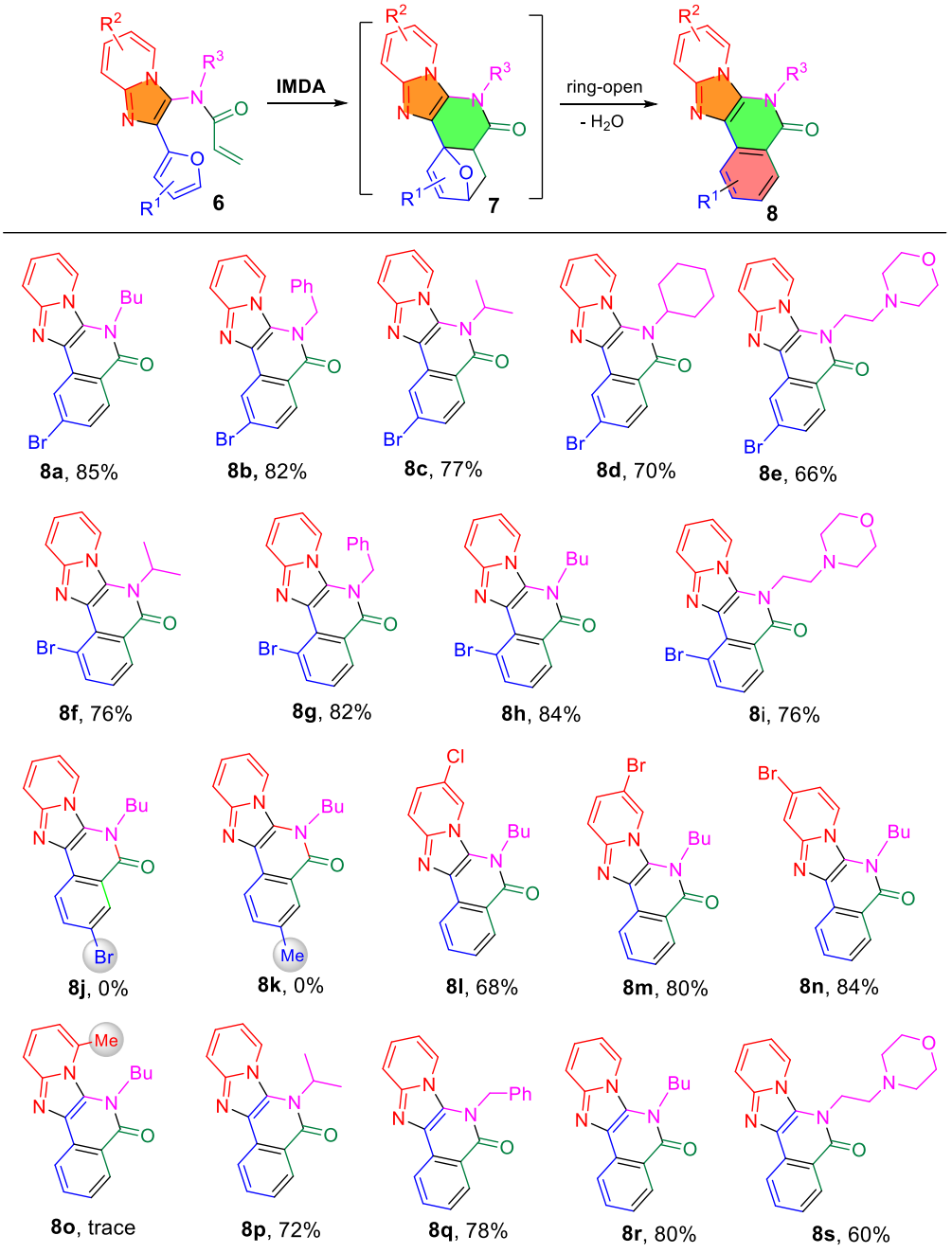

[a] Reaction conditions: **6** and $AlCl_3$ (10 mol%) in 1,2-dichlorobenzene at 180 °C for 4 h.

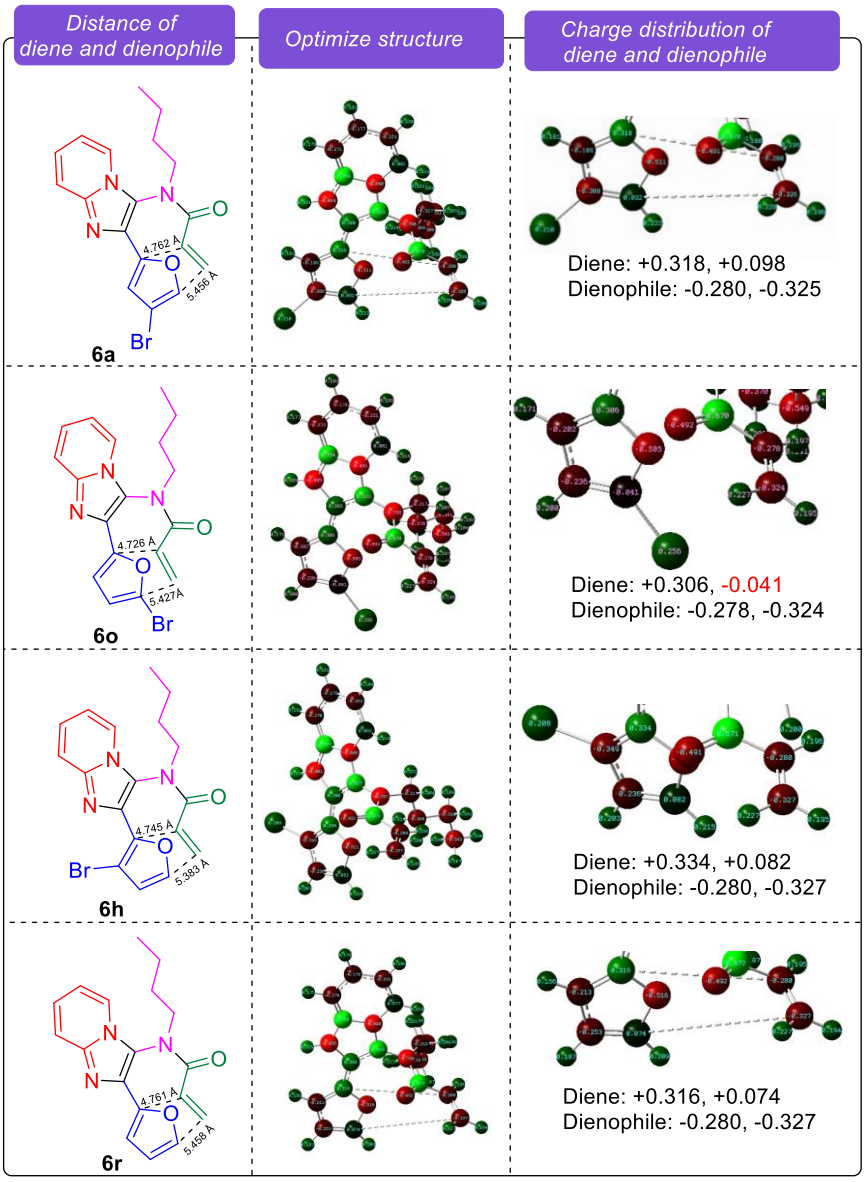

Figure 2. Transition state analysis of IMDA for **6a, 6o, 6h** and **6r**

The R^2 substituent on the imidazopyridine in **6** was found to have a significant electronic impact on the IMDA cycloaddition. When R^2 is a halogen (Br or Cl), it withdraws electron density through its inductive (-I) effect to increase diene reactivity for the cycloaddition to form **7**. For example, **8l** (R^2 = 5-Cl, 68%), **8m** (R^2 = 5-Br, 80%), and **8n** (R^2 = 4-Br, 84%) are high-yielding substrates. But an electron-donating group in **8o** (R^2 = 6-methyl) lowers the dienophilic nature and gave no product. The R^3 substituent from azonitriles is an important factor in forming intermediates **7** and promoting dehydrative aromatization for making products **8**. The reactions of R^3 as *n*-butyl resulted in the high yielding formation of **8a, h, l, m, n** and **r** 68–85%; R^3 as phenyl resulted in **8b, g** and **q** in 78–82% yields. R^3 is a bulky group that gave a reduced yield, R^3 as isopropyl and cyclopentene gave **8c, f, p** and **d** greater than70% yields. R^3 as *2*-morpholinoethyl gave **8e**, **i** and **s** in 60–76% yields.

Energy status for the transformation of compounds **6a** to **8a** was calculated using Gaussian 16

software (Figure 3) [20]. The *N*-acylated compound **6a** has a baseline relative energy of 0 kJ/mol, while the transition state of DA (TS-DA) reaction presents the highest energy barrier at 1.221 kJ/mol. The DA adduct shows a little lower energy at 1.001 kJ/mol, indicating a smooth transition from the transition state to the product. The final dehydrative ring-opening gives products by decreasing energy to 0.978 kJ/mol. Computational analysis indicates that the IMDA step has a high energy barrier which needs a catalyst, while the dehydrative re-aromatization step is energetically favorable.

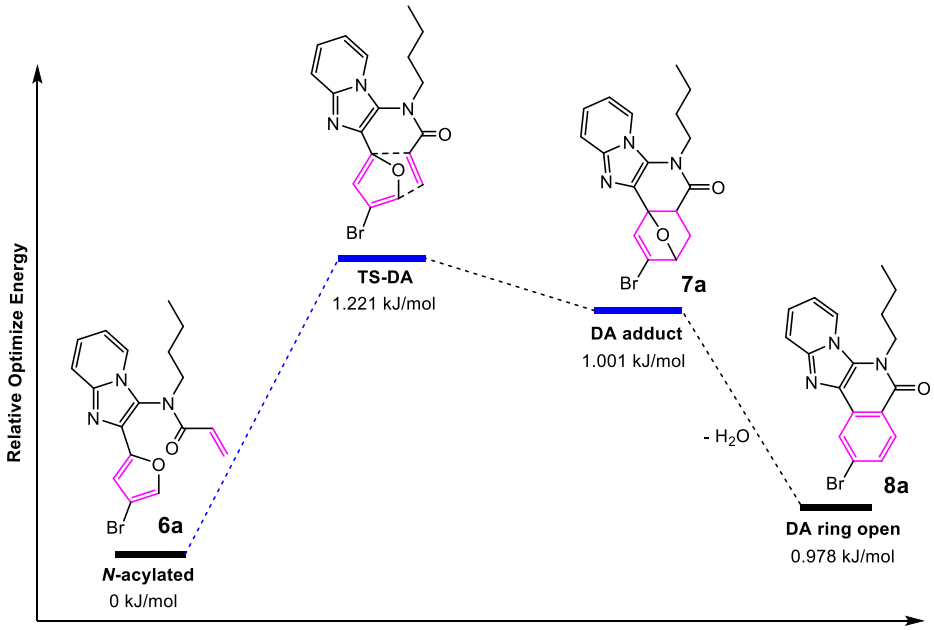

Figure 3. Relative energy diagram for the synthesis **8a** from **6a**

Other than furfural, thiophene-2-carbaldehyde **2s** was used for the GBB and *N*-acylation reactions to make **6t** (Scheme 4). The IMDA reaction of **6t** was carried out under the catalysis of $AlCl_3$ in dichlorobenzene at 180 °C for up to 24 h. But no compounds **7t** and **8t** were detected by LC-MS from the reaction mixture. The X-ray structure of **6t** indicated that the diene and dienophile are perpendicular to each other which prevents them from being properly aligned for the IMDA reaction. The transition state of the IMDA is electronically destabilized by the sulfur-group of thiophene to reduce diene's reactivity or altering the electrophilicity of the dienophile.

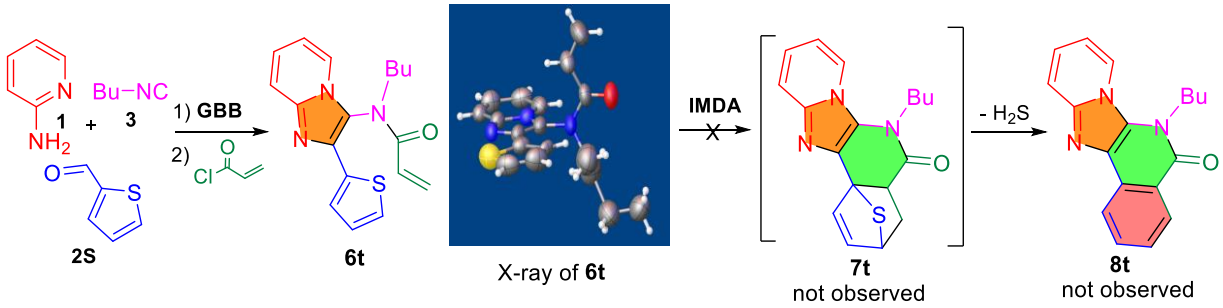

Scheme 4: Using thiophene-2-carbaldehyde for the synthesis of **8t**

Based on the computational analysis of the transition states, reaction mechanisms for IMDA and dehydration re-aromatization process are proposed in Scheme 5. In the IMDA reaction for making intermediate **7**, the carbonyl oxygen interacts with $AlCl_3$, enhancing electrophilicity and promoting the rearrangement to form stable oxonium ions. The removal of water from **7** is facilitated by protonation, producing reactive carbocations which undergo dehydrative aromatization to produce products **8**.

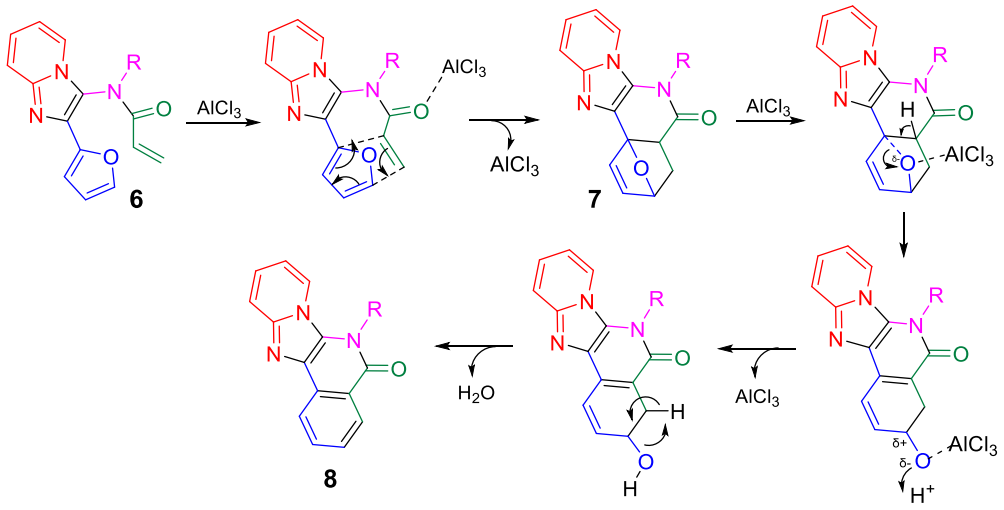

Scheme 5. Proposed mechanisms for IMDA and dehydration re-aromatization

Conclusions

In summary, we developed a reaction sequence involving GBB, *N*-acylation, IMDA and dehydrative re-aromatization reactions for the synthesis of imidazopyridine-fused isoquinolinones. Computational study of the IMDA reaction indicated that the position of R^1 group on the furan ring and R^2 group on the imidazopyridine have direct electronic impact on the IMDA reaction. This integrated reaction process provided a new avenue for making heterocyclic scaffolds with potential biological interest.

Experimental

General procedures for the synthesis of intermediates **4** and **6**

The GBB reactions for making imidazo[1,2-*a*]pyridines **4** were conducted using aminopyridines **1** (0.5 mmol), isocyanides **3** (0.6 mmol, 1.2 equiv.), and furfuraldehyde **2** (0.6 mmol, 1.2 equiv.) in 3:1 DCM/MeOH (4 mL) with $Yb(OTf)_3$ (0.04 mmol, 0.08 equiv.) as a Lewis acid catalyst under microwave irradiation at 100 °C for 1 h (Scheme 2, Table S1). Nineteen distinct adducts **4** were

obtained in 89–98% yields. The reactions of GBB adducts **4** with acryloyl chloride **5** (1.5 equiv.) in the presence of Et_3N (2 equiv.) at room temperature in anhydrous CH_2Cl_2 for 6 h afforded 19 *N*-acylated compounds **6** in 80–90% yields after flash chromatography with 1:6 EtOAc/hexanes (Scheme 2, Table S2) [18].

General procedures for the synthesis of products **8**

In the presence of 0.08 equiv. of Lewis's acid $AlCl_3$, *N*-acylation products **6** (0.1 mmol) in dichlorobenzene were heated at 180 °C for 4 h (Table 2). The reaction mixtures were checked by LC-MS to follow the formation of DA adducts **7** and the ring opening products **8** (Figure S1). After 4 h, the reaction mixtures were worked up and the crude products were purified by flash chromatography with 30:70 EtOAc/hexanes. Product structures were confirmed by ^{1}H- and ^{13}C-NMR analysis and x-ray crystal structure analysis of **8a**.

Density Functional Theory (DFT) Calculation

DFT computations were conducted utilizing Gaussian16W with the B3LYP functional and the 6-31G(d,p) basis set [20,21] . Geometry optimizations were performed without symmetry restrictions, and frequency analyses verified that all structures represented genuine minima. Charge distributions and interatomic distances were evaluated to determine reaction feasibility, utilizing GaussView for molecular visualization.

Supporting Information

Supporting Information File 1

General reaction procedures, compound characterization data, and copies of NMR spectra.

Data Availability Statement

The data underlying this study are available in the published article and its Supporting Information to this article

AUTHOR INFORMATION

Notes

The authors declare no competing financial interest.

References:

1. Krasavin, M.; Dar'in, D.; Balalaie, S. *Tetrahedron Lett.* **2021**, *86*, 153521. doi.org/10.1016/j.tetlet.2021.153521
2. Shen, G. B.; Yu, T.; Zhang, Y. L.; Ma, L. P.; Chen, L.; Lu, J. J.; Meng, T. *J. Heterocycl. Chem.* **2018**, *55* (4), 814–820. doi.org/10.1002/jhet.3102
3. Qian, Z.; Yang, A.; An, W.; Yu, T.; Wang, X.; Zhang, Y.; Shen, J.; Meng, T. *RSC Adv.* **2014**, *4* (92), 50947–50949. doi.org/10.1039/C4RA09196E
4. Tang, L.; Ren, J.; Ma, Y.; Wang, X.; Chen, L.; Shen, J.; Chen, Y.-L.; Xiong, B. *Tetrahedron Lett.* **2016**, *57* (21), 2311–2314. doi.org/10.1016/j.tetlet.2016.04.050
5. Srinivasulu, V.; Khanfar, M.; Omar, H. A.; ElAwady, R.; Sieburth, S. M.; Sebastian, A.; Zaher, D. M.; Al-Marzooq, F.; Hersi, F.; Al-Tel, T. H. *J. Org. Chem.* **2019**, *84* (22), 14476–14486. doi.org/10.1021/acs.joc.9b01919
6. Tandi, M.; Sharma, V.; Gopal, B.; Sundriyal, S. *RSC Adv.* **2025**, *15* (2), 1447–1489. doi.org/10.1039/d4ra06681b
7. Domling, A.; Wang, W.; Wang, K. *Chemical Rev.* **2012**, *112* (6), 3083–3135. doi.org/10.1021/cr100233r
8. Flores-Reyes, J. C.; Islas-Jácome, A.; González-Zamora, E. *Org. Chem. Front.* **2021**, *8* (19), 5460–5515. doi.org/10.1039/D1QO00313E
9. Slobbe, P.; Ruijter, E.; Orru, R. V. *Med. Chem. Commun.* **2012**, *3* (10), 1189–1218. doi.org/10.1039/C2MD20089A
10. Cai, Q.; Liu, M.-C.; Mao, B.-M.; Xie, X.; Jia, F.-C.; Zhu, Y.-P.; Wu, A.-X. *Chin. Chem. Lett.* **2015**, *26* (7), 881–884. doi.org/10.1016/j.cclet.2014.12.016
11. Erhorn, S. Zolpidem, In *xPharm: The Comprehensive Pharmacology Reference*, Enna, S.J., Bylund, D. B., Elsevier. **2007**; pp 1–5. doi.org/10.1016/B978-008055232-3.62888-0
12. Schneier, F. R.; Carrasco, J. L.; Hollander, E.; Campeas, R.; Fallon, B.; Saoud, J. B.; Feerick, J.; Liebowitz, M. R. *J. Clin. Psychopharmacol*. **1993**, *13* (2), 150–153. doi.org/10.1097/00004714-199304000-00011
13. Devi, N.; Rawal, R. K.; Singh, V. *Tetrahedron* **2015**, *71* (2), 183–232. doi.org/10.1016/j.tet.2014.10.032
14. Boltjes, A.; Dömling, A. *Eur. J. Org. Chem.* **2019**, *2019* (42), 7007-7049. doi.org/10.1002/ejoc.201901124
15. Veljkovic, I.; Zimmer, R.; Reissig, H.-U.; Bruedgam, I.; Hartl, H. *Synthesis* **2006**, *2006* (16), 2677–2684. doi.org/10.1055/s-2006-942506
16. Kesteleyn, B. R. R.; Schepens, W. B. G., HIV inhibiting 3, 4-dihydro-imidazo[4,5-B]pyridin-5-ones. Google Patents: 2011.

17. Lu, Q.; Huang, X.; Song, G.; Sun, C.-M.; Jasinski, J. P.; Keeley, A. C.; Zhang, W. *ACS Comb. Sci.* **2013**, *15* (7), 350–355. doi.org/10.1021/co400026s
18. Paulvannan, K.; Stille, J. R. *J. Org. Chem.* **1992**, *57* (20), 5319–5328. doi/10.1021/jo00046a011
19. Rae, R. L.; Żurek, J. M.; Paterson, M. J.; Bebbington, M. W. *Org. Biomol. Chem.* **2013**, *11* (45), 7946–7952. doi.org/10.1039/C3OB41616J
20. Frisch, M. J.; Trucks, G. W.; Schlegel, H. B.; Scuseria, G. E.; Robb, M. A.; Cheeseman, J. R.; Scalmani, G.; Barone, V.; Petersson, G. A.; Nakatsuji, H.; Li, X.; Caricato, M.; Marenich, A. V.; Bloino, J.; Janesko, B. G.; Gomperts, R.; Mennucci, B.; Hratchian, H. P.; Ortiz, J. V.; Izmaylov, A. F.; Sonnenberg, J. L.; Williams; Ding, F.; Lipparini, F.; Egidi, F.; Goings, J.; Peng, B.; Petrone, A.; Henderson, T.; Ranasinghe, D.; Zakrzewski, V. G.; Gao, J.; Rega, N.; Zheng, G.; Liang, W.; Hada, M.; Ehara, M.; Toyota, K.; Fukuda, R.; Hasegawa, J.; Ishida, M.; Nakajima, T.; Honda, Y.; Kitao, O.; Nakai, H.; Vreven, T.; Throssell, K.; Montgomery Jr., J. A.; Peralta, J. E.; Ogliaro, F.; Bearpark, M. J.; Heyd, J. J.; Brothers, E. N.; Kudin, K. N.; Staroverov, V. N.; Keith, T. A.; Kobayashi, R.; Normand, J.; Raghavachari, K.; Rendell, A. P.; Burant, J. C.; Iyengar, S. S.; Tomasi, J.; Cossi, M.; Millam, J. M.; Klene, M.; Adamo, C.; Cammi, R.; Ochterski, J. W.; Martin, R. L.; Morokuma, K.; Farkas, O.; Foresman, J. B.; Fox, D. J. *Gaussian 16 Rev. C.01*, Wallingford, CT, **2016**.
21. Ali, M. A.; Nath, A.; Islam, M. M.; Shaheed, S. B.; Dibbo, I. N. *RSC Adv.* **2022**, *12* (18), 11255–11261. doi.org/10.1039/D2RA00450J